Static and Dynamic Nuclear Magnetic Resonance Studies of Complexes of Trimethylplatinum(IV) Halides with Olefinic Thio- and Seleno-ethers. *X*-Ray Crystal Structures of [$PtXMe_3$(MeSeCH=CHSeMe)] (X = Cl or I)†

Edward W. Abel, Suresh K. Bhargava, Keith G. Orrell,* Andrew W. G. Platt, and Vladimir Šik
Department of Chemistry, University of Exeter, Exeter EX4 4QD
T. Stanley Cameron
Department of Chemistry, Dalhousie University, Halifax B3 4J3, Canada

Complexes of general type [$PtXMe_3$(MeECH=CHEMe)] (E = S or Se; X = Cl, Br, or I) have been isolated and their solution and solid-state structures established. Static structures in solution were characterised by ^1H, ^{13}C, ^{77}Se, and ^{195}Pt n.m.r. parameters; the dynamic stereochemistry of these complexes, arising from low-temperature chalcogen inversion and high-temperature fluxional rearrangements, was studied quantitatively by variable-temperature ^1H n.m.r. spectroscopy. Correlations were found between ^{195}Pt and ^{77}Se chemical shifts, and between ^{195}Pt shifts and ^1J(PtSe) values in these complexes. ^1J(CPt) values can be interpreted in terms of *trans* influence effects. The solution invertomer populations are very halogen- and temperature-dependent. In the case of selenium complexes, the predominant invertomer in solution corresponds to the single solid-state configuration as determined by *X*-ray crystallography. For the chloro-complex this is the *meso*-1 form and for the iodo-complex the *meso*-2 species. The effects of π-conjugation on the energies of the chalcogen inversion and platinum-methyl scrambling processes are discussed by comparing $\Delta G^{\ddagger}$ (298.15 K) values with those for analogous complexes with aliphatic and aromatic chalcogen ligands.

In earlier studies[1,2] on the structural dynamics of transition-metal complexes with Group 6B ligands, we have shown that complexes of trimethylplatinum(IV) halides with aliphatic dithio-, diseleno-, and thio/seleno-ethers of general type [$PtXMe_3$($MeECH_2CH_2E'Me$)] (X = Cl, Br, or I; E = E′ = S or Se and E = S, E′ = Se) are highly stereochemically non-rigid, exhibiting temperature-variable n.m.r. spectra over a wide temperature range (often exceeding 100 °C). Similar observations were made for complexes with aromatic dichalcogen ether ligands,[3] namely [$PtXMe_3$(*o*-$MeEC_6H_4EMe$)] (E = E′ = S, X = Cl; E = S, E′ = Se, X = Cl, Br, or I). However, the rates of chalcogen inversion and other fluxional processes were significantly different in the two classes of complexes to suggest an influence of ligand backbone on the stereodynamics of these mononuclear platinum(IV) complexes. In order to explore further this effect we have now synthesised analogous complexes with olefinic ligands, namely [$PtXMe_3$(MeECH=CHE′Me)] (E = E′ = S or Se; X = Cl, Br, or I). π-Electron conjugation effects have previously been shown to influence strongly the rates of pyramidal chalcogen inversion in rhenium(I) complexes[4] {*e.g.* [$ReX(CO)_3L$]}, and palladium(II) and platinum(II) complexes[5] (*e.g.* [PdX_2L] and [PtX_2L]) with similar ether ligands (L). We therefore wished to investigate whether similar influences were operating in these platinum(IV) complexes, and whether the high-temperature fluxional rearrangements, which are known to exist in these complexes, are also affected.

As these complexes, particularly those with selenium ligands, possess a variety of important n.m.r. nuclei, *e.g.* ^1H, ^{13}C, ^{77}Se, and ^{195}Pt, we have carried out a multinuclear investigation on the low-temperature solutions of these complexes in order to characterise precisely the invertomer mixtures which arise. *X*-Ray crystallographic studies on some of these complexes have been used to ascertain whether the predominant structural isomer in solution can be closely identified with the solid-state structure.

Experimental

Materials.—The ligands *cis*-1,2-bis(methylthio)ethene and *cis*-1,2-bis(methylseleno)ethene were prepared by reported methods.[6,7]

The complexes were all prepared by the same general method. The preparation of [$PtBrMe_3$(MeSeCH=CHSeMe)] described below may be taken as typical.

A slight excess of 1,2-bis(methylseleno)ethene (0.216 g, 0.57 mmol) in chloroform (3 cm^3) was added to trimethylplatinum bromide (0.125 3 g, 0.4 mmol) in chloroform (5 cm^3) and the resulting solution heated to reflux for 2 h. The solution was concentrated under vacuum to *ca.* 1 cm^3, and light petroleum (b.p. 40—60 °C; 1 cm^3) was added to precipitate a white solid. The solvent was removed and the product recrystallised from chloroform–light petroleum (b.p. 40—60 °C) to yield white crystals of [1,2-bis(methylseleno)ethene]bromotrimethylplatinum(IV) (0.190 g, 91%).

In view of the larger amounts of complex required for ^{13}C and ^{77}Se n.m.r. studies, interconversions of complexes by halogen-exchange reactions were also achieved in order to minimise the quantities of starting materials. Thus, the chloride and bromide complexes were prepared from the iodide complex by reaction of the latter with the appropriate silver halide as described previously.[8]

All the complexes were white or pale yellow crystals which were readily soluble in common organic solvents. They were quite stable both in air and in solution. Analytical data are reported in Table 1.

N.M.R. Spectra.—Hydrogen-1, ^{13}C, and ^{77}Se spectra were obtained at 100.0, 25.1, and 19.1 MHz respectively on a JEOL PS/PFT-100 spectrometer in this Department operating in the

† [1,2-Bis(methylseleno)ethene]chloro- and [1,2-bis(methylseleno)-ethene]iodo-trimethylplatinum(IV).

Supplementary data available (No. SUP 56081, 4 pp.): thermal parameters. See Instructions for Authors, *J. Chem. Soc., Dalton Trans.*, 1985, Issue 1, pp. xvii—xix. Structure factors are available from the editorial office.

Table 1. Characterisation of the complexes [$PtXMe_3$(MeECH=CHEMe)]

Complex	Colour	M.p. (°C)	Analysis[a] (%) C	H
(1) [$PtClMe_3$(MeSCH=CHSMe)]	White	185—187	21.25 (21.20)	4.35 (4.30)
(2) [$PtBrMe_3$(MeSCH=CHSMe)]	White	190[b]	19.10 (19.05)	3.90 (3.90)
(3) [$PtIMe_3$(MeSCH=CHSMe)]	Pale yellow	191—192[b]	17.25 (17.25)	3.50 (3.55)
(4) [$PtClMe_3$(MeSeCH=CHSeMe)]	White	170	17.15 (17.10)	3.45 (3.45)
(5) [$PtBrMe_3$(MeSeCH=CHSeMe)]	White	168	15.75 (15.50)	3.20 (3.10)
(6) [$PtIMe_3$(MeSeCH=CHSeMe)]	Pale yellow	161	14.45 (14.45)	2.95 (2.85)

[a] Calculated values are in parentheses. [b] Decomposes.

Fourier-transform mode. Probe temperature control was as previously described.[2] Platinum-195 spectra were obtained at 19.3 MHz on a JEOL FX 90Q spectrometer at the City of London Polytechnic. All the complexes were dissolved in CD_2Cl_2 for low-temperature n.m.r. studies, while $C_6D_5NO_2$ or $C_6D_5NO_2$–C_6D_6 were used as solvents in the high-temperature range (*ca.* 30—165 °C).

Bandshape analyses of the ^1H spectra were carried out using our version of the original DNMR3 program of Kleier and Binsch.[9]

X-*Ray Structure Determinations.*—Single-crystal structure determinations of [$PtXMe_3$(MeSeCH=CHSeMe)] (X = Cl or I), compounds (**4**) and (**6**), were obtained.

Crystal data for (**4**). $C_7H_{17}ClPtSe_2$, M = 489.7, orthorhombic, a = 12.146(2), b = 23.093(4), c = 9.219(2) Å, space group $Pbca$, Z = 8, D_c = 2.515 g cm^{-3}, Mo-K_α radiation (λ = 0.7093 Å), μ = 16.7 mm^{-1}.

Crystal data for (**6**). $C_7H_{17}IPtSe_2$, M = 581.1, monoclinic, a = 11.962(4), b = 13.843(3), c = 8.126(2) Å, β = 99.85(2)°, space group $P2_1/n$, Z = 4, D_c = 2.910 g cm^{-3}, Mo-K_α radiation, μ = 18.4 mm^{-1}.

A Picker four-circle diffractometer was used to obtain 768 and 1 345 independent observable reflections with $I > 3\sigma(I)$ for (**4**) and (**6**) respectively; 2 976 (**4**) and 3 195 (**6**) (h,k,l) reflections were scanned in the range $3 \leqslant 2\theta \leqslant 55°$. Crystals of dimensions 0.1 × 0.2 × 0.33 and 0.1 × 0.12 × 0.13 mm were used; Lorentz, polarisation, and absorption corrections were applied. The structures were solved by Patterson and Fourier methods[10] and were refined by full-matrix least squares to R = 0.052 (**4**) and 0.047 (**6**) with anisotropic thermal parameters for all non-hydrogen atoms; weights were given by $w^{-1} = \sigma^2(F_o) + 0.001(F_o)^2$. The olefinic hydrogen atoms only could be located, and the positions of these were not refined.

Results

Static N.M.R. Parameters.—The two sulphur or selenium atoms in these five-membered ring complexes are chiral centres and thus, in the absence of any internal exchange process, four diastereoisomers (two distinct *meso* forms and a degenerate pair of DL forms) may exist (Figure 1). This is totally analogous to the situation existing for the homochalcogen-aliphatic[2] and -aromatic[3] ligand complexes. The presence of these individual isomers (strictly termed, invertomers, as they arise from the cessation of pyramidal inversion of the E atoms) is clearly shown in the low-temperature ^1H n.m.r. spectra.

The complex [$PtClMe_3$(MeSCH=CHSMe)], whose 400-MHz ^1H spectrum at −80 °C is shown in Figure 2, may be taken as representative of all the other complexes. The spectrum consists of four main regions of absorption. The sulphur-methyl region (ii) consists of four signals (plus ^{195}Pt satellites) due to the three distinct invertomers. On warming the sample to *ca.* −10 °C these signals coalesce to a single signal (plus ^{195}Pt satellites) due to the onset of pyramidal sulphur inversion. In the platinum-methyl regions (iii/iv) at low temperature, seven signals (plus ^{195}Pt satellites) are expected and indeed detected at 400 MHz. The three resonances due to Pt methyls *trans* to halogen occur at lower frequencies (δ 0.6—0.9), region (iv), and with larger $^2J(^{195}Pt–H)$ values (72.3—74.0 Hz) compared to those for Pt-methyls *trans* to chalcogen (δ 1.1—1.2, ^2J = 66.0—70.6 Hz), region (iii). These trends were noted originally in aliphatic chalcogen-ether complexes[1,2] and are useful assignments in the present complexes. Full proton chemical shift and ^2J(Pt–H) data for these complexes in the slow- and fast-inversion limits are presented in Table 2. No attempt was made to assign individual Pt-methyl signals since this region was not subsequently used for dynamic n.m.r. analysis despite the gross changes (*viz.*, seven lines coalescing to two) which occurred on warming to higher temperatures.

The ligand olefinic region (i) (Figure 2) also showed the presence of all invertomers at low temperature. Two singlets at δ 6.82 and 6.84 with ^3J(Pt–H) values of 14.5 and 14.0 Hz respectively were assigned to the *meso*-1 and *meso*-2 isomers respectively, while an AB quartet centred at δ 6.75 ($\Delta\nu_{AB}$ = 0.121 p.p.m., $^2J_{AB}$ = 7.0 Hz) was due to the DL pair. This region of the spectrum was also not examined in further detail because of the very small chemical shift differences involved, and because no additional information to that obtained from the complete analyses of the ligand-methyl region would ensue.

Full assignments of the ligand-methyl region of the spectra were made, prior to performing a dynamic n.m.r. bandshape analysis. Assignments for the selenium ligand complexes are shown in Figure 3 and the proton parameters for all the static complexes are given in Table 3. Assignments were made on the basis of previously observed trends[2] in chemical shifts, ^3J(Pt–H) values, and invertomer populations. The two signals (neglecting ^{195}Pt satellites) at lower frequencies were assigned to methyl c (DL) and methyls dd′ (*meso*-2). The signals at higher frequencies were accordingly assigned to methyls aa′ (*meso*-1) and methyl b (DL).

An examination of the trends in Figure 3 and Table 3 shows that an increase in halogen mass/size favours the less sterically hindered *meso*-2 and DL isomers at the expense of *meso*-1. The same trend was previously observed for the saturated ligand complexes, the main difference between the two series of complexes being that in the olefinic ligand complexes the abundances of the DL species are considerably lower, the usual order of populations being *meso*-1 > *meso*-2 ≫ DL-1 = DL-2. By contrast, the usual order for the aliphatic ligand complexes was *meso*-1 > DL-1 = DL-2 ≫ *meso*-2, although in the case of the iodo-complex the DL isomers became the most abundant species. The halogen dependencies of the invertomer populations for the two series of complexes are displayed graphically in Figure 4.

Carbon-13 parameters. The ^{13}C chemical shifts and one- and two-bond ^{13}C–^{195}Pt coupling constants are given in Table 4. The labelling of the methyl carbons is shown in Figure 5. The trends in both chemical shifts and coupling constants are exactly analogous to those observed in the aliphatic ligand complexes, [$PtXMe_3$($MeSeCH_2CH_2SeMe$)].[8] In both series the expected dependence of chemical shifts on electronegativity of the halogen is followed for Pt-methyl (*trans* E) carbons with δ(Cl) > δ(Br) > δ(I) but this trend is reversed for ligand-methyl and Pt-methyl (*trans* X) carbons. As far as the methyl-

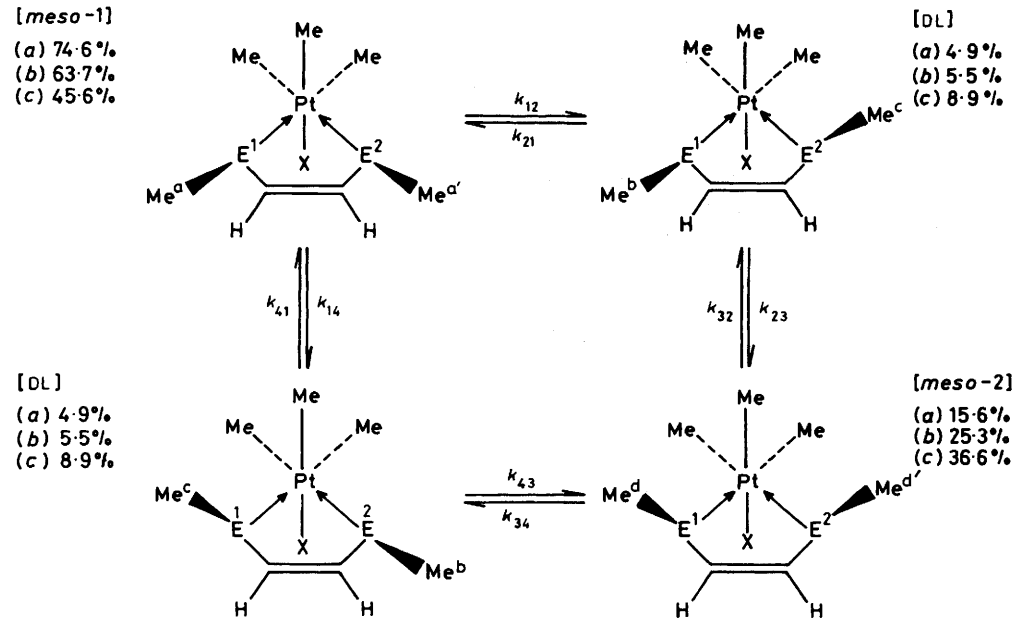

Figure 1. Interconversion of *meso* and DL isomers of [$PtXMe_3$(MeECH=CHEMe)]. Percentage populations refer to the complexes when E = S, (*a*) X = Cl, (*b*) X = Br, and (*c*) X = I at *ca.* −76 °C; Me^a—Me^d refer to the E-methyl environments

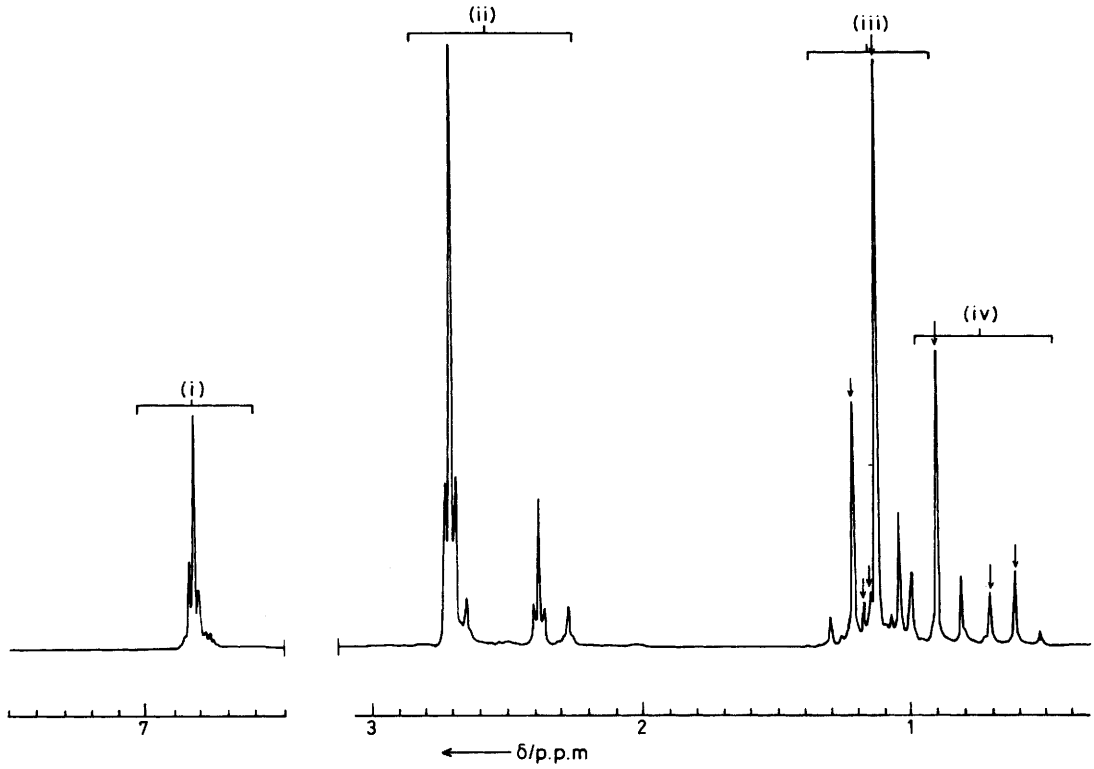

Figure 2. Hydrogen-1 n.m.r. spectrum (400 MHz) of [$PtClMe_3$(MeSCH=CHSMe)] in CD_2Cl_2 at −80 °C. The arrows in regions (iii/iv) indicate the main Pt-methyl signals. All lines not arrowed in these regions are ^{195}Pt satellites

carbon–platinum-195 coupling constants are concerned, $^1J_{CPt}$(*trans* X) values are invariably greater than $^1J_{CPt}$(*trans* E). The variation of ^1J(*trans* X) with halogen follows the trend expected by the *trans* influence,[11,12] with values decreasing by approximately 3% from chloro- to iodo-complexes. Within a given complex, the magnitudes of $^1J_{CPt}$(*trans* X) showed no simple dependence on invertomer, while values of $^1J_{PtC}$(*trans* Se) were invariably greater in *meso*-1 than *meso*-2 implying stronger Pt–C bonds and weaker Pt–Se bonds in *meso*-1 compared to *meso*-2.

The $^2J_{PtC}$ values are expected to reflect changes in the Pt–Se bond strengths. However, the few values recorded in Table 4 do not indicate any significant trend. Difficulties in interpreting $^2J_{CPt}$ values were similarly encountered in the aliphatic ligand complexes.[8]

Selenium-77 and platinum-195 parameters. It is notable that

Table 2. Chemical shifts and spin coupling constants of platinum-methyl protons in the slow- and fast-inversion limits[a]

		Pt–Me(*trans* to E)		Pt–Me(*trans* to X)	
Complex	θ_c/°C	δ/p.p.m.	$^2J^b$/Hz	δ/p.p.m.	$^2J^b$/Hz
(1)	−80.0	1.21, 1.17, 1.15, 1.13	65.81, 70.00, 68.00, 70.23	0.90, 0.70, 0.61	73.91, 74.22, 73.00
	−15.1	1.23	70.56	0.87	72.30
(2)	−74.9	1.35, 1.31, 1.28, 1.16	69.58, 70.55, 70.07, 71.0	1.08, 0.89, 0.79	72.88, 72.11, 72.78
	8.4	1.33	70.68	0.95	72.28
(3)	−74.5	1.48, 1.46, 1.36, 1.34	70.31, 71.00, 69.80, 69.60	1.20, 1.04, 0.95	70.70, 69.96, 70.70
	8.0	1.50	71.6	1.07	69.60
(4)	−55.8	1.40, 1.37, 1.31, 1.28	69.58, 69.83, 69.82, 69.82	1.08, 0.80, 0.72	73.74, 73.98, 73.72
	77.7	1.37	71.05	0.86	73.61
(5)	−46.8	1.47, 1.45, 1.44, 1.41	69.83, 70.07, 70.20, 70.20	1.15, 0.90, 0.82	72.51, 72.76, 73.61
	60.5	1.46	70.81	0.93	72.02
(6)	−46.7	1.61, 1.59, 1.58	70.80, 70.31, 71.04	1.05, 0.96, 0.94	70.80, 71.30, 70.80
	77.7	1.62	71.30	1.05	71.04

[a] Chemical shifts are relative to $SiMe_4$. The solvent for sulphur complexes was CD_2Cl_2, and for selenium complexes $CDCl_3$. [b] $^2J(^{195}Pt–C–^1H)$.

Table 3. Static parameters of the ligand methyl protons in the complexes $[PtXMe_3(MeECH{=}CHEMe)]$

		meso-1 isomer			DL isomers						*meso*-2 isomer			
X	E	ν_a[a]	$^3J^b$	p^c	ν_b	^3J	p	ν_c	^3J	p	ν_d	^3J	p	T_2^*/s
Cl	S	276.97	13.92	0.746	270.60	12.10	0.049	233.76	13.68	0.049	244.26	15.86	0.156	0.212
Br	S	285.16	14.52	0.637	279.90	12.94	0.055	233.03	13.92	0.055	243.89	15.87	0.253	0.230
I	S	298.21	15.63	0.456	293.82	13.60	0.089	232.66	14.04	0.089	243.04	16.11	0.366	0.232
Cl	Se	269.80	10.74	0.518	261.50	9.80	0.086	219.72	11.22	0.086	231.40	12.45	0.310	0.205
Br	Se	275.02	11.23	0.405	267.94	10.38	0.112	216.43	11.35	0.112	227.17	12.32	0.371	0.300
I	Se	289.60	12.20	0.178	283.20	11.72	0.120	217.30	11.24	0.120	228.00	12.70	0.582	0.198

[a] Chemical shifts (ν_i/Hz) of E methyls measured relative to $SiMe_4$. [b] $^3J(^{195}Pt–E–C–^1H)$/Hz. [c] Isomer population (±0.005).

Table 4. Methyl ^{13}C n.m.r. data[a] for $[PtXMe_3(MeSeCH{=}CHSeMe)]$

	meso-1						DL								*meso*-2					
X	δ(C[1])	^1J	δ(C[2])	^1J	δ(C[3])	^2J	δ(C[1])	^1J	δ(C[2])	^1J	δ(C[3])	^1J	δ(C[4])	^2J	δ(C[5])	^2J	δ(C[1])	^1J	δ(C[2])	^1J	δ(C[3])	^2J
Cl	−6.1	682.4	1.8	628.7	10.6	5.6	−5.7	686.0	1.2	632.3	1.4	629.9	11.4	9.8	9.4	*b*	−3.6	688.5	2.4	626.5	7.8	*b*
Br	−1.1	676.3	1.0	622.5	12.2	7.3	−1.3	676.2	0.4	636.0	0.4	623.3	13.0	4.9	4.9	*b*	0.5	682.4	1.1	618.9	8.1	*b*
I	5.6	666.0	−0.4	633.0	15.7	9.8	7.4	—	−1.8	620.3	−1.3	617.1	16.4	9.0	10.2	*b*	7.2	660.2	−1.4	621.3	8.8	*b*

[a] At −40 °C in $CDCl_3$. Shifts are to high frequency of $SiMe_4$; J values are in Hz. [b] Not measured.

Table 5. Selenium-77 and ^{195}Pt n.m.r. data[a] for $[PtXMe_3(MeSeCH{=}CHSeMe)]$

	meso-1				DL						*meso*-2			
X	p^b	δ(Pt)	δ(Se)	^1J	p^b	δ(Pt)	δ(Se[1])	^1J	δ(Se[2])	^1J	p^b	δ(Pt)	δ(Se)	^1J
Cl	51.5	1 311.6	305.4	330.1	25.2	1 127.9	323.1	337.7	300.7	244.2	23.3	1 276.6	299.5	246.6
Br	35.5	1 204.0	299.1	339.9	28.1	985.5	319.4	346.7	296.3	256.8	36.4	1 104.1	298.0	256.6
I	28.0	1 001.6	286.1	353.5	23.5	729.8	310.6	361.6	287.4	271.5	48.5	807.1	295.0	283.0

[a] In $CDCl_3$. Platinum-195 shifts to high frequency of 21.4 MHz at 0 °C. Selenium-77 shifts to high frequency of $SeMe_2$ at −30 °C. [b] Invertomer populations are appreciably temperature dependent such that $p_\theta = p_{0\,°C} + x(\theta/°C)$, where x = 0.13 (*meso*-1), 0.10 (DL), and −0.23 (*meso*-2).

the ^{77}Se and ^{195}Pt chemical shifts are significantly greater than those pertaining to the corresponding saturated ligand complexes (*cf.* Table 3 of ref. 8). This is presumably a result of the differing anisotropies associated with C–C and C=C bonds. In the case of the unsaturated ligand complexes, Table 5 reveals several unusual features. In particular, the ^{195}Pt shifts for the DL species are to lower frequency of the shifts in the *meso* invertomers whereas in all other S/Se saturated ligand species studied to date[8] this signal lies between the two *meso* values. The temperature dependences of the DL shifts (*ca.* 0.5 p.p.m. $°C^{-1}$) were also markedly higher than those of the *meso* shifts (*ca.* 0.02—0.1 p.p.m. $°C^{-1}$), and caused broadening and apparent splitting of the signals in some cases, as a result of temperature gradients in the sample probably caused by ^1H decoupling.

Linear plots of δ(Se) *versus* δ(Pt) and $^1J_{SePt}$ *versus* δ(Pt) within each invertomer species were found to hold as in the case of $[PtXMe_3(MeSeCH_2CH_2SeMe)]$.[8] Figure 6 illustrates the linear relationships of δ(Se) and δ(Pt) for the invertomers of $[PtXMe_3(MeSeCH{=}CHSeMe)]$ (X = Cl, Br, or I).

The trends in chemical shifts and coupling constants are generally as observed previously[8] with increasing electro-

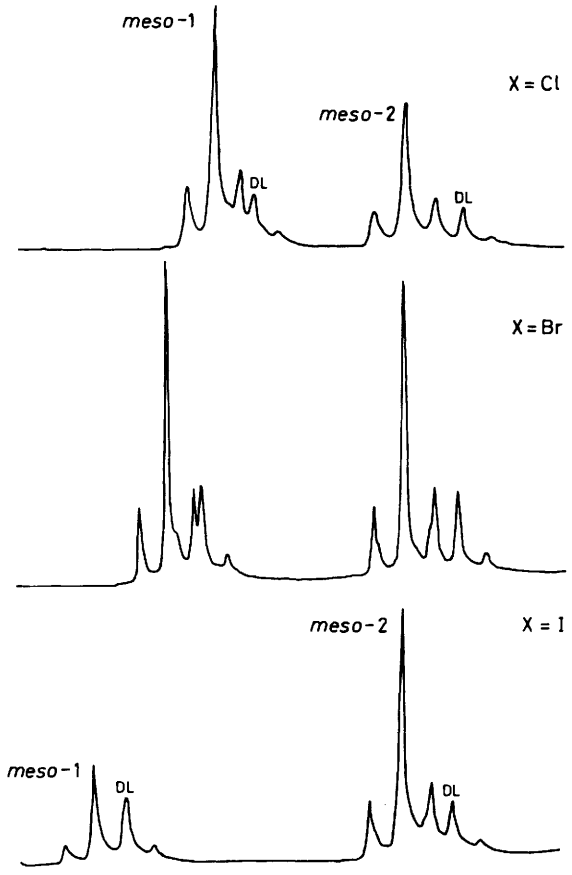

Figure 3. Ligand-methyl ^{1}H spectra of [$PtXMe_3$(MeSeCH=CHSeMe)] showing the halogen dependence of invertomer populations

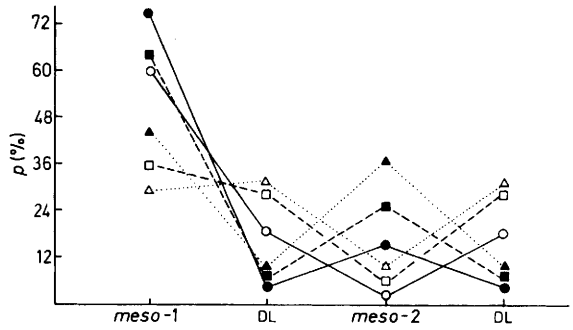

Figure 4. Variation of invertomer population with halogen and ligand backbone in the complexes [$PtXMe_3$(MeSRSMe)]: R = –CH=CH–, X = Cl (●), Br (■), or I (▲); R = $-CH_2CH_2-$, X = Cl (○), Br (□), or I (△)

negativity of the halogen causing deshielding of a magnetic environment, with a corresponding decrease in $^1J_{SePt}$. It should also be noted that, for a given invertomer, the values of $^1J_{SePt}$ are invariably higher than in the corresponding saturated ligand analogues. This would appear to reflect differing strengths of Pt–Se bonds as seemed to be the case for [$PtXMe_3$\{MeSe-$(CH_2)_n$SeMe\}] (n = 2 or 3). Accordingly, $MeSeCH_2CH_2SeMe$ would *not* be expected to displace the unsaturated analogue from its complexes: equation (1). However, equation (1) lies well

$$[PtXMe_3(MeSeCH{=}CHSeMe)] + MeSeCH_2CH_2SeMe \longrightarrow [PtXMe_3(MeSeCH_2CH_2SeMe)] + MeSeCH{=}CHSeMe \quad (1)$$

to the right and occurs rapidly at room temperature. The ligand $MeSe(CH_2)_3SeMe$ reacts in a similar fashion. It thus appears that the Pt–Se bonds in these unsaturated ligand complexes are relatively weak for mononuclear complexes, and $^1J_{SePt}$ values are not direct reflections of these bond strengths. Changes in $^1J_{SePt}$ values may be primarily due to non-bonded electron-pair interactions which mask smaller effects caused by changes in bond strength.

A particularly notable feature of these systems is the pronounced dependence of invertomer populations on temperature (Table 5, footnote *b*). This is in contrast to saturated ligand complexes which are essentially temperature independent.[2,8] This variation is particularly evident in the ^{195}Pt spectra and its magnitude depends only on the type of invertomer and not on the halogen. Temperature decrease causes a decrease in *meso*-1 and DL abundances with a corresponding increase in *meso*-2 abundance. The effect of lowering the temperature will be slightly to shorten bond lengths, and presumably the invertomer populations depend rather critically on this. Shortening bond lengths is likely to increase interaction between ligand methyls and platinum methyls (*trans* X) or halogen X, depending on which isomer is considered. Changes in populations should reflect the relative importance of these interactions. Since a decrease in temperature produces an increase in *meso*-2 population, ligand methyl–halogen interactions would seem to dominate the changes in population. However, the lack of any dependence on halogen type for this population change is difficult to rationalise.

X-Ray Data.—The low-temperature n.m.r. results indicated a changeover in the predominant invertomer in solution from *meso*-1 to *meso*-2 as the halogen size increased. It was therefore of considerable interest to examine which solid-state configurations existed for different halogen complexes. The complexes [$PtClMe_3$(MeSeCH=CHSeMe)] (**4**) and [$PtIMe_3$(MeSeCH=CHSeMe)] (**6**) were chosen for *X*-ray analysis since they displayed the greatest difference in invertomer mixtures in solution (see Figure 3 and Table 3).

The atomic co-ordinates for complexes (**4**) and (**6**) are given in Tables 6 and 7, and the stereoscopic views of the structures are shown in Figures 7 and 8. In the chloro-derivative (**4**), the Se–Me groups are clearly on the same side of the five-membered ring as the chlorine atom (*cf. meso*-1 invertomer) while in the iodo-derivative (**6**), these groups are on the opposite side of the ring to the iodine atom (*cf. meso*-2 invertomer). These results strikingly illustrate how the predominant invertomer of these Se complexes in solution becomes the sole invertomer in the solid state. A similar trend is to be expected for the sulphur ligand complexes although this has not been confirmed to date. The different relative orientations of the SeMe groups in complexes (**4**) and (**6**) are reflected in the different mean torsional angles X–Pt–Se–Me, being 25(2)° for (**4**) and 175(6)° for (**6**). The rings in the two compounds also differ slightly. That in compound (**4**) is distinctly non-planar with the platinum atom 0.66 Å from the least-squares best plane through the other four atoms which themselves deviate by < 0.01 Å from the plane, while the ring in compound (**6**) is essentially planar (maximum and mean deviations of 0.018 and 0.012 Å from the least-squares best plane through all five atoms).

The mean Pt–C, Pt–Cl, and Pt–I distances of 2.06(3), 2.440(9), and 2.791(2) Å are within the range of expected values. The mean Pt–Se distance of 2.531(3) Å lies between two recently observed values for this bond length, 2.598(7) Å in

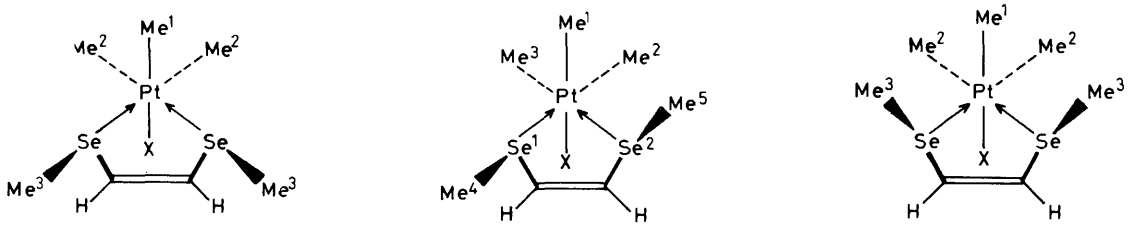

Figure 5. Labelled invertomer species of [$PtXMe_3$(MeSeCH=CHSeMe)]

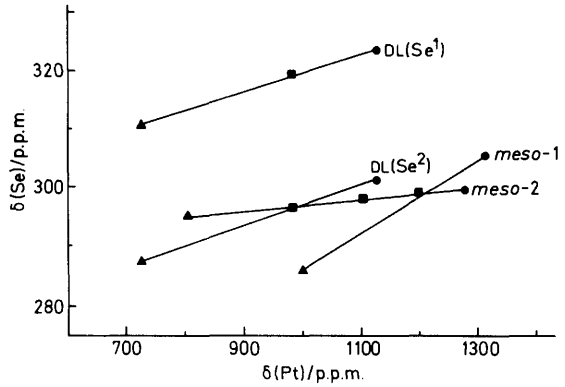

Figure 6. Correlation of ^{77}Se and ^{195}Pt shifts for invertomers of [$PtXMe_3$(MeSeCH=CHSeMe)]: X = Cl (●), Br (■), or I (▲)

$[(PtBrMe_3)_2(SeMe_2)_2]$[13] and 2.426(3) Å in $[Pt(Se_2CNBu^i_2)_2]$.[14] Full details of bond distances and angles in complexes (**4**) and (**6**) are given in Table 8.

Dynamic N.M.R. Data.—Chalcogen inversion energies were computed by examining the ligand-methyl regions of the ^1H spectra. The signals coalesce with increasing temperature according to the scheme in Figure 1. The case of [$PtClMe_3$-(MeSCH=CHSMe)] is depicted in Figure 9 (N.B.: in this case, the DL signals are scarcely visible in the temperature range shown). Theoretical bandshapes were computed according to the cyclic scheme for the interchanging E methyls shown below

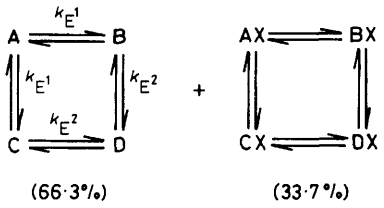

(X = ^{195}Pt). It will be noted that only single-site inversion is considered as previously[2,8] and two different magnitudes of rate constant k_{E^1} and k_{E^2} are included to allow for the different kinetic pathways *meso*-1 ⟶ DL and DL ⟶ *meso*-2. The spectra were found to be sensitive to *both* rate constants at most temperatures and gave more satisfactory fits with theoretical spectra based on pairs of k values rather than on single k values (Figure 9). Theoretical spectra were based on the static ^1H parameters in Table 3. Arrhenius and Eyring plots of the 'best fit' spectra yielded the energy data in Table 9.

At temperatures well above those at which sulphur or selenium inversion had become rapid, additional spectral changes were observed. These involved broadening, and

Table 6. Atomic co-ordinates for [$PtClMe_3$(MeSeCH=CHSeMe)] (**4**)

Atom	x	y	z
Pt	0.161 03(9)	0.118 09(6)	0.101 09(15)
Se(1)	0.042 8(3)	0.206 9(2)	0.141 6(3)
Se(2)	0.007 9(3)	0.085 3(2)	−0.065 1(4)
Cl	0.264 2(8)	0.164 6(5)	−0.093 9(10)
C(1)	0.249 5(33)	0.042 8(17)	0.068 9(36)
C(2)	0.279 1(24)	0.141 4(19)	0.255 7(41)
C(3)	0.086 5(25)	0.077 7(16)	0.270 6(38)
C(4)	0.128 1(29)	0.274 2(15)	0.061 3(38)
C(5)	−0.055 7(23)	0.204 2(13)	−0.015 2(38)
C(6)	−0.065 0(22)	0.157 1(16)	−0.094 6(30)
C(7)	0.070 9(30)	0.073 6(16)	−0.257 1(45)
H(5)	−0.106 3(0)	0.243 2(0)	−0.041 4(0)
H(6)	−0.121 9(0)	0.159 7(0)	−0.190 4(0)

Table 7. Atomic co-ordinates for [$PtIMe_3$(MeSeCH=CHSeMe)] (**6**)

Atom	x	y	z
Pt	0.220 83(7)	0.101 16(6)	0.376 78(10)
I	0.309 22(15)	0.258 72(13)	0.570 75(18)
Se(1)	0.196 51(20)	0.219 59(17)	0.135 91(26)
Se(2)	0.422 92(18)	0.076 31(18)	0.329 76(28)
C(1)	0.241 4(20)	0.005 5(18)	0.583 5(33)
C(2)	0.057 4(18)	0.128 6(17)	0.428 5(28)
C(3)	0.148 1(19)	−0.015 0(19)	0.235 1(31)
C(4)	0.115 4(21)	0.160 8(20)	−0.069 6(27)
C(5)	0.342 3(20)	0.218 7(16)	0.076 5(24)
C(6)	0.430 0(19)	0.163 3(18)	0.146 2(26)
C(7)	0.436 3(21)	−0.043 0(19)	0.203 5(32)
H(5)	0.356 3(0)	0.269 0(0)	−0.022 4(0)
H(6)	0.509 2(0)	0.168 5(0)	0.094 2(0)

eventual coalescence of the two Pt-methyl signals to one singlet (plus ^{195}Pt satellites). This change was perfectly reversible with temperature and, in view of the retention of ^{195}Pt–methyl coupling, was due to an intramolecular rearrangement of Pt-methyl environments. Exactly analogous changes have been reported for saturated ligand ring complexes of platinum(IV).[3,8,15,16] In the case of mononuclear platinum(IV) complexes[3,8] this scrambling process accompanied a 180° 'pancake' rotation of the ligand moiety. However, it has not always proved possible to confirm the separate existence of the 'pancake' rotation process and the energy barrier of this process has been assumed[3] to be the same as that of the Pt-methyl scrambling. We are forced to make the same assumption in the present complexes, where again we postulate a highly non-rigid pseudo-eight-co-ordinate platinum intermediate associated with the ligand rotation process, such a species possessing incipient methyl scrambling. More recent studies[17] with Pt^{IV} complexes of the ligand 2,4,6-trithiaheptane, $MeSCH_2SCH_2S$-Me, have provided direct confirmatory evidence for a ligand 'pancake' rotation in Pt^{IV} complexes and yielded reliable energy

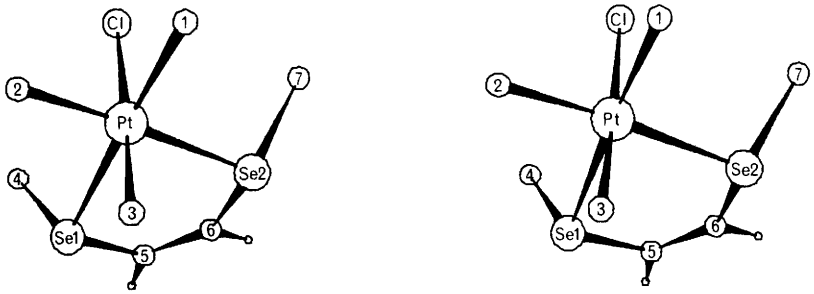

Figure 7. Stereoview of *X*-ray structure of [$PtClMe_3$(MeSeCH=CHSeMe)]

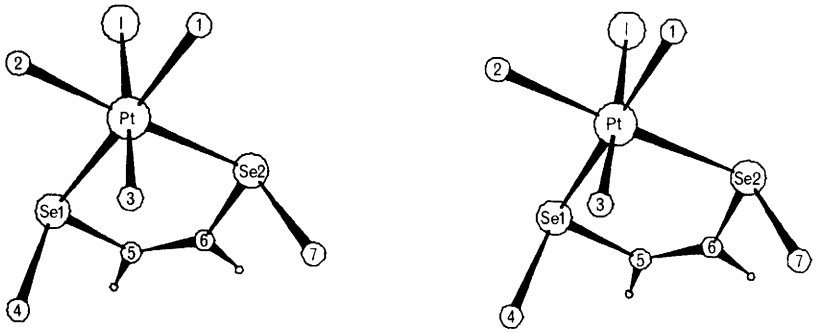

Figure 8. Stereoview of *X*-ray structure of [$PtIMe_3$(MeSeCH=CHSeMe)]

Table 8. Bond distances (Å) and angles (°) for [$PtClMe_3$(MeSeCH=CHSeMe)] (**4**) and [$PtIMe_3$(MeSeCH=CHSeMe)] (**6**)

(*a*) Bond distances

	(4)	(6)		(4)	(6)
Pt–X	2.440(9)	2.791(2)	Se(1)–C(4)	2.01(4)	1.96(2)
Pt–Se(1)	2.532(4)	2.531(2)	Se(1)–C(5)	1.88(3)	1.89(2)
Pt–Se(2)	2.525(4)	2.535(3)	Se(2)–C(6)	1.90(4)	1.93(2)
Pt–C(1)	2.07(4)	2.12(2)	Se(2)–C(7)	1.95(3)	1.97(3)
Pt–C(2)	2.09(3)	2.10(2)	C(5)–C(6)	1.32(5)	1.34(3)
Pt–C(3)	2.03(3)	2.08(2)			

(*b*) Bond angles

	(4)	(6)		(4)	(6)
X–Pt–Se(1)	92.5(3)	85.00(7)	C(1)–Pt–C(2)	88(2)	86.6(9)
X–Pt–Se(2)	93.6(3)	84.97(7)	C(1)–Pt–C(3)	87(1)	86.4(11)
X–Pt–C(1)	89.9(10)	93.4(7)	C(2)–Pt–C(3)	84(2)	86.3(9)
X–Pt–C(2)	92.0(11)	91.2(6)	Pt–Se(1)–C(4)	106(1)	111.4(8)
X–Pt–C(3)	175.6(9)	177.5(7)	Pt–Se(1)–C(5)	103(1)	101.8(6)
Se(1)–Pt–C(1)	176.8(11)	178.3(8)	C(4)–Se(1)–C(5)	94(1)	97.1(10)
Se(1)–Pt–C(2)	94.6(11)	92.9(6)	Pt–Se(2)–C(7)	108(1)	110.9(7)
Se(1)–Pt–C(3)	90.3(10)	95.8(8)	Pt–Se(2)–C(6)	100(1)	101.6(7)
Se(2)–Pt–C(1)	92.5(11)	92.9(7)	C(6)–Se(2)–C(7)	100(1)	96(1)
Se(2)–Pt–C(2)	174.3(11)	176.1(6)	Se(1)–C(5)–C(6)	121(2)	126(2)
Se(2)–Pt–C(3)	90.0(10)	97.5(5)	Se(2)–C(6)–C(5)	127(2)	123(2)

data for the process. The assumption of ligand rotation initiating Pt-methyl scrambling in the present complexes is therefore well founded.

Computation of high-temperature bandshapes of the Pt-methyl signals was carried out in the usual way, using the static parameters given in Table 10. The resulting energy data are tabulated in Table 11.

Pyramidal Inversion.—Most of the data in Table 9 are in accordance with expectations from previous studies. Values of $\Delta S^{\ddagger}$ are close to 0 J K^{-1} mol^{-1} and $\log_{10}$ (A/s^{-1}) values are *ca.* 13, both parameters therefore being supportive of purely intramolecular processes. Pyramidal inversion of Se atoms occurs less readily that at S atoms ($\Delta\Delta G^{\ddagger}$ *ca.* 10 kJ mol^{-1}) as has been noted previously.[2,3,15,16] However, the main purpose of the present work was to examine relative rates of inversion in unsaturated and saturated ligand complexes. The relevant data for comparison are included in Table 9. Replacement of an aliphatic backbone by an olefinic backbone consistently reduces the $\Delta G^{\ddagger}$ values for the chalcogen inversion by 9—15 kJ mol^{-1}. Comparisons are made slightly more difficult by the fact that the $\Delta G^{\ddagger}$ values for the saturated ligand complexes were based on single rate-constant fittings.[2] The pairs of data for E^1 and E^2 inversion in the present complexes essentially reflect the different ground-state populations of the *meso*-1 and DL species. The lowering of $\Delta G^{\ddagger}$ values on introducing unsaturation into the ligand can almost certainly be attributed to (3*p*–2*p*)π or (4*p*–2*p*)π conjugation between the chalcogen

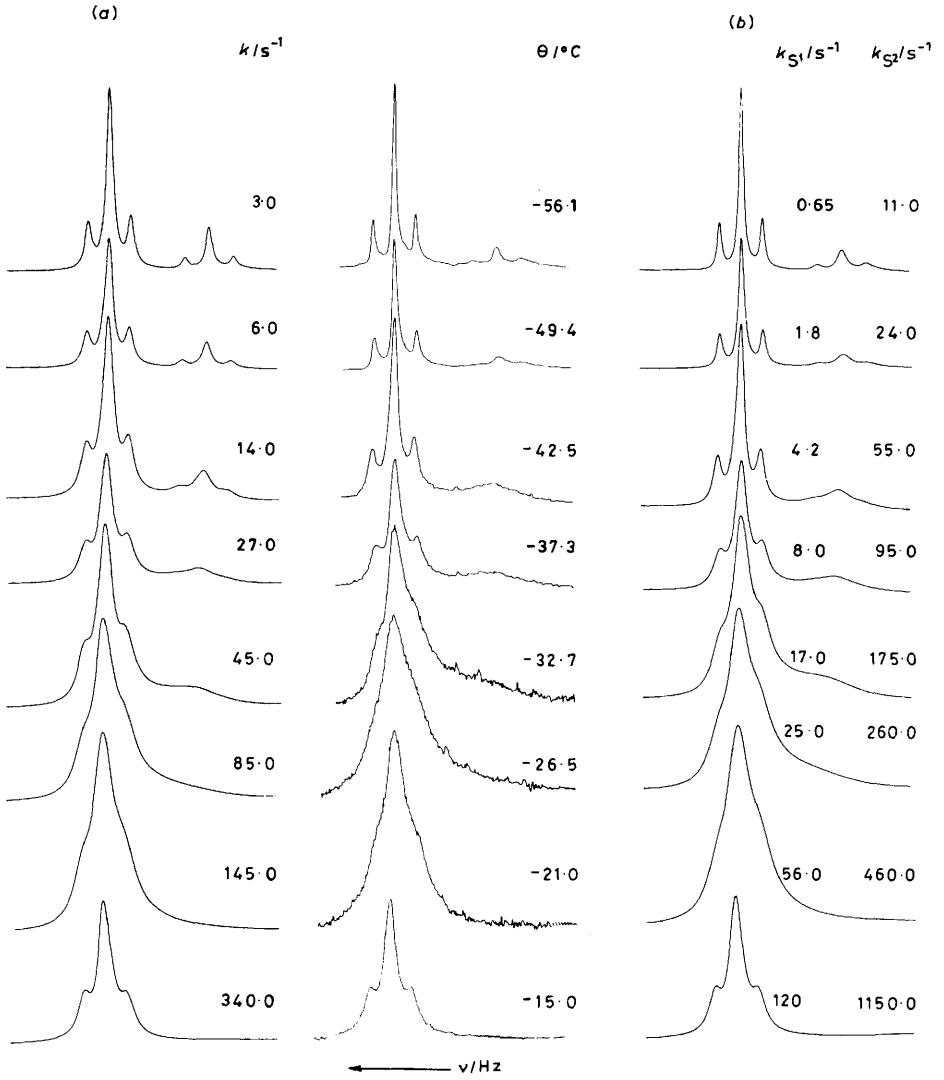

Figure 9. Experimental and computer-synthesised ^1H spectra of [$PtClMe_3$(MeSCH=CHSMe)] (ligand-methyl region) showing the effects of using (*a*) one and (*b*) two independent rate constants to simulate the S inversion

Table 9. Arrhenius and activation parameters[a] for sulphur and selenium inversion in the homochalcogen ligand complexes of trimethylplatinum(IV) halides

Complex	Inversion[b]	E_a/kJ mol^{-1}	$\log_{10} A$	$\Delta G^{\ddagger}$/kJ mol^{-1}	$\Delta H^{\ddagger}$/kJ mol^{-1}	$\Delta S^{\ddagger}$/J K^{-1} mol^{-1}
[$PtClMe_3$(MeSCH=CHSMe)]	S^1	57.9 ± 1.4	13.7 ± 0.3	52.4 ± 0.3	55.9 ± 1.4	11.8 ± 6.0
	S^2	50.8 ± 1.6	13.2 ± 0.4	48.1 ± 0.4	48.8 ± 1.6	2.4 ± 6.8
[$PtClMe_3$($MeSCH_2CH_2SMe$)]	S[c]	63.4 ± 0.7	12.8 ± 0.1	63.3 ± 0.1	61.0 ± 0.7	−7.7 ± 2.4
[$PtBrMe_3$(MeSCH=CHSMe)]	S^1	56.4 ± 0.5	13.3 ± 0.1	53.4 ± 0.1	54.3 ± 0.5	3.1 ± 2.2
	S^2	50.2 ± 1.9	13.0 ± 0.4	48.6 ± 0.5	48.2 ± 1.9	−1.5 ± 8.3
[$PtBrMe_3$($MeSCH_2CH_2SMe$)]	S[c]	69.8 ± 2.2	14.0 ± 0.4	62.8 ± 0.1	67.4 ± 2.2	15.5 ± 7.5
[$PtIMe_3$(MeSCH=CHSMe)]	S^1	58.6 ± 2.6	13.6 ± 0.6	53.8 ± 0.8	56.7 ± 2.6	9.6 ± 11.3
	S^2	55.5 ± 1.8	14.1 ± 0.4	47.8 ± 0.8	53.6 ± 1.8	19.4 ± 7.9
[$PtIMe_3$($MeSCH_2CH_2SMe$)]	S[c]	66.9 ± 2.0	13.5 ± 0.3	62.6 ± 0.0	64.4 ± 2.0	5.9 ± 6.5
[$PtBrMe_3$(MeSeCH=CHSeMe)]	Se^1	64.4 ± 1.3	12.9 ± 0.2	63.4 ± 0.1	62.0 ± 1.3	−4.5 ± 4.4
	Se^2	62.2 ± 0.5	13.2 ± 0.1	60.1 ± 0.1	59.7 ± 0.6	−1.0 ± 1.8
[$PtBrMe_3$($MeSeCH_2CH_2SeMe$)]	Se[c]	77.3 ± 4.2	13.6 ± 0.7	72.4 ± 0.3	74.6 ± 4.2	7.3 ± 13.0

[a] At 298.15 K. [b] S^1, Se^1: [*meso*-1] ⟶ [DL-1]. S^2, Se^2: [DL-1] ⟶ [*meso*-2]. [c] Ref. 2.

lone pair and the ligand backbone, the interactions being more effective in the planar transition state that in the ground state, and the $(3p–2p)\pi$ interaction for S atoms being marginally more pronounced than the $(4p–2p)\pi$ interaction for Se atoms.

Similar results were obtained in *cis*-platinum(II) and -palladium(II) complexes of type *cis*-[MX_2L] [X = Cl, Br, or I; L = $MeSCH_2CH_2SMe$, *o*-$(SMe)_2C_6H_3Me$, or *cis*-MeSCH=CHSMe].[5] The change here on going from aliphatic

Table 10. Static parameters used in calculating platinum-methyl scrambling energy barriers in the complexes [$PtXMe_3$(MeEREMe)]

				Pt–Me (*trans* to S or Se)		Pt–Me (*trans* to X)		T_2^*/s	
X	E	R	θ/°C	ν[a]/Hz	^2J[b]/Hz	ν[a]/Hz	^2J[b]/Hz	Main bands	Pt satellites
Cl	S	–CH=CH–	27.0	144.0[c]	70.56	88.86	72.27	0.344	0.344
Cl	S	$-CH_2CH_2-$[d]	71.2	136.23[e]	70.30	77.88	72.27	0.286	0.240
Br	Se	–CH=CH–	60.5	146.24[e]	70.81	93.38	72.02	0.143	0.143
Br	Se	$-CH_2CH_2-$[d]	91.6	154.8[e]	70.56	84.22	71.53	0.160	0.143

[a] Chemical shifts measured relative to $SiMe_4$. [b] $^2J(^{195}Pt–C–^1H)$. [c] In $CDCl_3$. [d] See ref. 1 for preparative details. [e] In $C_6D_5NO_2$–C_6D_6.

Table 11. Energy barriers[a] calculated for platinum-methyl scrambling in the homochalcogen ligand complexes

Complex	E_a/kJ mol^{-1}	$\log_{10} A$	$\Delta G^‡$/kJ mol^{-1}	$\Delta H^‡$/kJ mol^{-1}	$\Delta S^‡$/J K^{-1} mol^{-1}
[$PtClMe_3$(MeSCH=CHSMe)]	87.3 ± 0.8	13.9 ± 0.1	80.4 ± 0.1	84.3 ± 0.8	13.1 ± 2.2
[$PtClMe_3$($MeSCH_2CH_2SMe$)][b]	91.7 ± 1.2	13.1 ± 0.2	90.0 ± 0.3	88.3 ± 1.2	−5.8 ± 2.9
[$PtBrMe_3$(MeSeCH=CHSeMe)]	75.9 ± 0.3	12.1 ± 0.1	79.7 ± 0.1	72.9 ± 0.3	−23.0 ± 0.7
[$PtBrMe_3$($MeSeCH_2CH_2SeMe$)][b]	86.3 ± 0.7	12.4 ± 0.1	88.2 ± 0.2	82.8 ± 0.6	−17.9 ± 1.5
[$PtClMe_3$(*o*-$MeSC_6H_4SMe$)][c]	83.6 ± 1.0	12.7 ± 0.1	83.8 ± 0.2	80.4 ± 0.1	−11.4 ± 2.5

[a] At 298.15 K. [b] See ref. 1 for preparative details. [c] Ref. 3.

to olefinic ligands was 10—12 kJ mol^{-1}, with the aromatic ligands having intermediate values. An analogous trend was also noted[4] in the two series of rhenium(I) complexes, [$ReX(CO)_3L$] (X = Cl, Br, or I; L = $MeECH_2CH_2EMe$ or MeECH=CHEMe, E = S or Se). Here the sulphur inversion barriers were lowered by 9—12 kJ mol^{-1} and the selenium barriers by 6—8 kJ mol^{-1}.

Fluxional Rearrangement.—The platinum-methyl scrambling data for the unsaturated ligand complexes are presented in Table 11 alongside comparisons with aliphatic- and aromatic-ligand data. The $\Delta G^‡$ values are *ca.* 20 kJ mol^{-1} higher than those of chalcogen inversion and are essentially independent of halogen. There appears to be a small dependence on ligand backbone with values for olefinic ligands being 8—10 kJ mol^{-1} lower than for aliphatic ligands, the aromatic ligand complex again being intermediate in magnitude. This is the same dependence that was found for the chalcogen inversion, and lends support to the two processes being at least indirectly related. It suggests that only when pyramidal inversion is sufficiently rapid will ligand rotation and platinum-methyl scrambling become possible. Thus, if the chalcogen inversion is facilitated by π–π conjugation then this will also act in favour of the platinum-methyl scrambling.

Acknowledgements

We are grateful to the S.E.R.C. for a postdoctoral research assistantship (to A. W. G. P.), and to the Commonwealth Scholarship Commission (U.K.) and the University Grants Commission (India) for support (to S. K. B.). We also gratefully acknowledge the use of the S.E.R.C. n.m.r. services at the City of London Polytechnic and the University of Warwick.

References

1 E. W. Abel, A. R. Khan, K. Kite, K. G. Orell, and V. Šik, *J. Chem. Soc., Dalton Trans.*, 1980, 1169.
2 E. W. Abel, A. R. Khan, K. Kite, K. G. Orrell, and V. Šik, *J. Chem. Soc., Dalton Trans.*, 1980, 1175.
3 E. W. Abel, S. K. Bhargava, K. Kite, K. G. Orrell, V. Šik, and B. L. Williams, *J. Chem. Soc., Dalton Trans.*, 1982, 583.
4 E. W. Abel, S. K. Bhargava, M. B. Bhatti, K. Kite, M. A. Mazid, K. G. Orrell, V. Šik, B. L. Williams, M. B. Hursthouse, and K. M. A. Malik, *J. Chem. Soc., Dalton Trans.*, 1982, 2065.
5 E. W. Abel, S. K. Bhargava, K. Kite, K. G. Orrell, V. Šik, and B. L. Williams, *Polyhedron*, 1982, **1**, 289.
6 F. R. Hartley, S. G. Murray, W. Levason, H. E. Soutter, and C. A. McAuliffe, *Inorg. Chim. Acta*, 1979, **35**, 265.
7 L. M. Kataeva, E. G. Kataeva, and D. Ya Idiyatullina, *Zh. Strukt. Khim.*, 1966, **7**, 380.
8 E. W. Abel, K. G. Orrell, and A. W. G. Platt, *J. Chem. Soc., Dalton Trans.*, 1983, 2345.
9 D. A. Kleier and G. Binsch, DNMR3 Program 165, Quantum Chemistry, Program Exchange, Indiana University, 1970.
10 D. F. Grant and E. J. Gabe, *J. Appl. Crystallogr.*, 1978, **11**, 114.
11 D. E. Clegg, J. R. Hall, and C. A. Swile, *J. Organomet. Chem.*, 1971, **38**, 403.
12 M. H. Chisholm, H, C. Clarke, L. E. Manzer, J. B. Stothers, and J. E. H. Ward, *J. Am. Chem. Soc.*, 1973, **95**, 8574.
13 E. W. Abel, A. R. Khan, K. Kite, K. G. Orrell, V. Šik, T. S. Cameron, and R. E. Cordes, *J. Chem. Soc., Chem. Commun.*, 1979, 713.
14 W-H. Pan, J. P. Fackler, and H-W. Chen, *Inorg. Chem.*, 1981, **20**, 856.
15 E. W. Abel, A. R. Khan, K. Kite, K. G. Orrell, and V. Šik, *J. Chem. Soc., Dalton Trans.*, 1980, 2208, 2220.
16 E. W. Abel, K. Kite, K. G. Orrell, V. Šik, and B. L. Williams, *J. Chem. Soc., Dalton Trans.*, 1981, 2439.
17 E. W. Abel, M. Z. A. Chowdhury, K. G. Orrell, and V. Šik, *J. Organomet. Chem.*, 1983, **258**, 109.

Received 23*rd March* 1984; *Paper* 4/475